Slope Efficiency Characteristics of Mode-hop Driven Tunable Single-mode Cholesteric Liquid Crystal Laser

Yo Inoue, Hiroyuki Yoshida, Kenta Inoue, Yusuke Shiozaki, Hitoshi Kubo,
Akihiko Fujii, and Masanori Ozaki
Department of Electrical, Electronic and Information Engineering, Osaka University,
Yamada-oka, Suita, Osaka 565-0871, Japan

ABSTRACT

We report tunable single-mode lasing with an improved slope efficiency from a cholesteric liquid crystal (ChLC) cavity with a three-layered structure. The device consists of one photopolymerized ChLC layer with a wide reflection band, another ChLC layer with a notch reflection band and a Rhodamine-6G-doped ionic liquid layer acting as the gain medium. Single-mode lasing can be obtained in this device structure because the ChLC layer with the notch reflection band strongly reflects only one of the Fabry-Perot cavity modes. Tuning of the lasing wavelength is achieved by tuning the reflection band of the notch ChLC. The device showed a maximum slope efficiency of 16%, which was found to be approximately 1.5 times larger than that of ordinary ChLC lasers doped with the pyrromethene 597 laser dye.

Keywords: cholesteric liquid crystal laser, slope efficiency, single-mode, tunable laser, DBR laser

1. INTRODUCTION

Cholesteric liquid crystals (ChLCs) are known to self-organize into helical structures with periodicities of a few hundred nanometers and thus possess a reflection band $\Delta\lambda$ (= Δnp) attributed to their periodicity p and birefringence Δn. By introducing a gain medium (usually dyes) with appropriate fluorescence properties, lasing can be realized in these materials. Consequently, ChLCs lasers have attracted a large amount of interest as compact, low-threshold, and tunable coherent light sources [1].

In periodic structures such as ChLCs, light with wavelengths within the reflection band is reflected, while light at the reflection band-edge wavelength is trapped inside, and either of these mechanisms can be employed to realize lasing. Lasers employing the former mechanism are called distributed Bragg reflector (DBR) lasers and the latter are called distributed feedback (DFB) lasers. To date, most studies have investigated the DFB-ChLC laser system in which the laser dye is directly doped in ChLCs[2-7], and only a few studies have investigated ChLC lasers with the DBR structure due to the difficulty of obtaining single-mode lasing in DBR-type laser system [8-9]. However, DBR-ChLC lasers in which the gain medium is separated from the ChLC cavity and the choice of luminescent materials is almost infinite, is expected to outperform DFB-ChLC lasers in terms of slope efficiency.

Lasing from DFB-ChLC lasers occur only at the edge-frequency of the reflection band and is strictly single-mode. On the other hand, DBR-ChLC lasers easily become multimode when the active layer is too thick because the number of the cavity modes depend on thickness and refractive index of the active layer based on the equation of cavity modes $m\lambda = 2nL$, where m is mode index, n is refractive index, and L is cavity length. However, an active layer thickness greater than 10 μm is desirable to obtain sufficient light absorption. We overcome this trade-off by using the ChLC Bragg reflector with a notch reflection band to select one of the cavity modes in a thick cell.

In order to ensure single-mode lasing in our DBR-ChLC laser device, we employ a three-layered structure consisting of one photopolymerized ChLC (PChLC) layer with a wide reflection band, a dye-doped ionic liquid active layer (an ionic liquid was used for its nonvolatility and ability to dissolve laser dyes), and another ChLC layer with a narrow reflection peak (notch-ChLC). Single-mode lasing can be obtained in this layered structure because the notch-ChLC layer strongly reflects only one of the Fabry-Perot cavity modes and the large difference of the lasing threshold is obtained between the unique mode and the other modes. The tuning of the lasing wavelength is possible by shifting the reflection band of the notch-ChLC to cause cavity mode hopping. In addition, because the ionic liquid used in the active

Liquid Crystals XV, edited by Iam Choon Khoo, Proc. of SPIE Vol. 8114, 811415

layer is isotropic, high quantum-yield laser dyes nonsoluble in ChLCs can be used; hence, the slope efficiency is improved. In this report, first, we simulated tunable single-mode lasing in the layered structure of the DBR-ChLC laser by finite-difference time-domain (FDTD) analysis. And then, lasing characteristics of the designed DBR-ChLC device is actually investigated.

2. SIMULATION

Here, tunable single-mode laser using notch-ChLC is simulated by FDTD method. In Fig. 1, schematic of DBR-type ChLC laser is shown. The active layer with 20 μm thickness is sandwiched between two right-handed ChLC layers with 4 μm thickness. The gain medium placed in the active layer is a four-level system with each energy level possessing electron densities of N_i (i=0, 1, 2, 3) m^{-3}, numbered in order from the bottom of the energy levels. The extraordinary (n_e) and ordinary (n_o) refractive indices of LC molecules are assigned to be 1.56 and 1.50 in the ChLC layer 1 and 1.70 and 1.50 in the ChLC layer 2, respectively, and refractive index of glass substrate with thickness of 1μm is 1.50. Perfectly matched layer (PML) is used as an absorbing boundary condition[10]. The extraordinary and ordinary dielectric constants of LC molecules are ε_e ($=n_e^2$) and ε_o ($=n_o^2$), and thus, the dielectric tensor $\tilde{\varepsilon}(x)$ to represent dielectric distribution of helix is described as

$$\tilde{\varepsilon}(x) = \begin{bmatrix} \varepsilon_o & 0 & 0 \\ 0 & \varepsilon_o + \Delta\varepsilon \sin^2\theta(x) & \Delta\varepsilon \sin\theta(x)\cos\theta(x) \\ 0 & \Delta\varepsilon \sin\theta(x)\cos\theta(x) & \varepsilon_o + \Delta\varepsilon \cos^2\theta(x) \end{bmatrix},$$

where $\Delta\varepsilon$ is the dielectric anisotropy ($=\varepsilon_e - \varepsilon_o$) and $\theta(x)$ is the angle between LC director and z-axis.

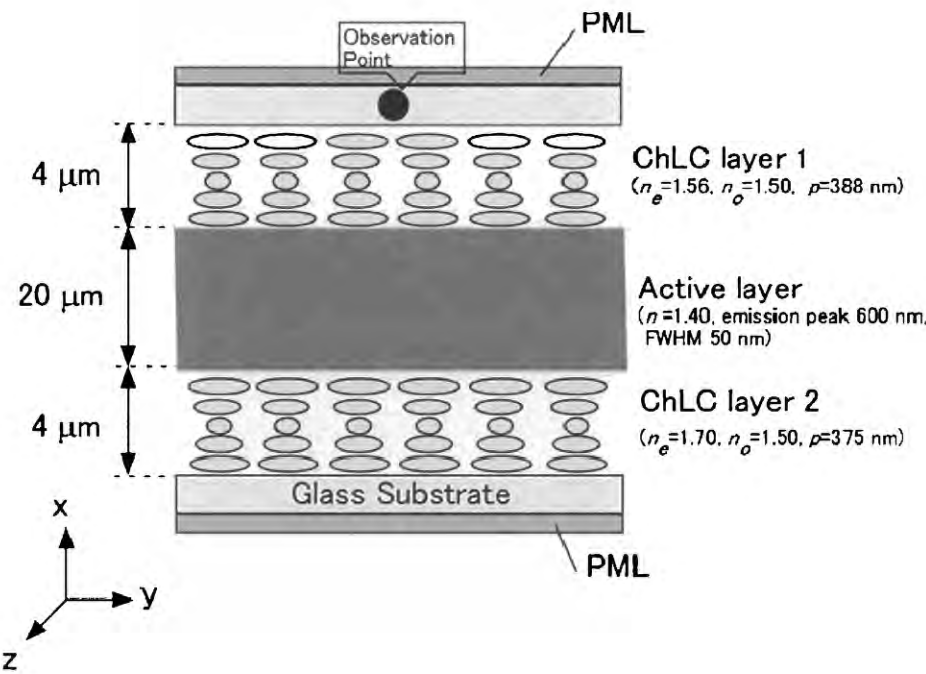

Fig. 1 Schematic of DBR-ChLC device

The time-dependant electromagnetic field along the x-axis is calculated by using Yee's FDTD algorism[11] to solve Maxwell's equation,

$$\nabla \times \mathbf{E}(x,t) = -\mu_0 \frac{\partial \mathbf{H}(x,t)}{\partial t}$$

$$\nabla \times \mathbf{H}(x,t) = \varepsilon_0 \tilde{\varepsilon}(x) \frac{\partial \mathbf{E}(x,t)}{\partial t} + \frac{\partial \mathbf{P}(x,t)}{\partial t},$$

where ε_0 and μ_0 are the dielectric permittivity and the magnetic permeability in vacuum, respectively. $\mathbf{P}(x,t)$ is the polarization density, generating radiation from the gain medium in the active layer. $\mathbf{P}(x,t)$ is described in the following Lorentz oscillator model,

$$\frac{d^2\mathbf{P}(x,t)}{dt^2} + \Delta\omega_a \frac{d\mathbf{P}(x,t)}{dt} + \omega_a{}^2 \mathbf{P}(x,t) = \frac{\gamma_r}{\gamma_c} \frac{e^2}{m} \Delta N(x,t) E(x,t),$$

where $\Delta\omega_a = \frac{1}{\tau_{21}} + \frac{2}{T_2}$ is the full width at half maximum (FWHM) line width of luminescence and at this time, $\Delta\lambda$ (= $2\pi c/\Delta\omega_a$) is set as 50 nm, a common value for organic laser dyes. τ_{ij} (i, j=0,1,2,3) is the transition i → j. T_2 is the mean time between dephasing events assigned to be 7.63×10^{-15} s. ω_a (= $2\pi c/\lambda_a$) is the central frequency of emission and λ_a (central wavelength of emission) is chosen to be 600 nm. $\Delta N(x,t)$ is the difference between electron numbers at levels 1 and 2, corresponding to $N_1(x,t) - N_2(x,t)$. $\gamma_r = 1/\tau_{21}$ and $\gamma_c = \frac{e^2}{m} \cdot \frac{\omega_a}{6\pi\varepsilon_0 c^3}$ are the classical rates related with radiation based on electron transition, e is the electron charge, m is the electron mass and c is the speed of light in vacuum.

The electron densities at each energy level (N_0, N_1, N_2, N_3) follow the rate equation,

$$\frac{dN_3(x,t)}{dt} = P_r N_0(x,t) - \frac{N_3(x,t)}{\tau_{32}}$$

$$\frac{dN_2(x,t)}{dt} = \frac{N_3(x,t)}{\tau_{32}} + \frac{1}{\hbar\omega_a} \mathbf{E}(x,t) \cdot \frac{\partial \mathbf{P}(x,t)}{\partial t} - \frac{N_2(x,t)}{\tau_{21}}$$

$$\frac{dN_1(x,t)}{dt} = \frac{N_2(x,t)}{\tau_{21}} + \frac{1}{\hbar\omega_a} \mathbf{E}(x,t) \cdot \frac{\partial \mathbf{P}(x,t)}{\partial t} - \frac{N_1(x,t)}{\tau_{10}}$$

$$\frac{dN_0(x,t)}{dt} = \frac{N_1(x,t)}{\tau_{10}} - P_r N_0(x,t),$$

where τ_{32}, τ_{21}, and τ_{10} are chosen to be 1×10^{-13}, 1×10^{-9}, 1×10^{-11} s, respectively. The total electron density $N_0{}^0 = N_0 + N_1 + N_2 + N_3$ is 1.2×10^{25} m^{-3}. P_r is the pumping rate of electrons from ground state N_0 to N_3, and is chosen to be 5×10^8 s^{-1}.

Figure 2 shows the transmittance spectra of ChLC layers 1 and 2 calculated at normal incidence of right-circularly polarized light by the Berreman's 4×4 matrix method[1]. While a wide reflection band with reflectance of almost 100% was observed in the ChLC layer 2, a notched reflection band with FWHM of approximately 35 nm was found in ChLC layer 1. In Fig. 3, lasing characteristics of the DBR-ChLC was simulated by FDTD method, and also for comparison, lasing characteristics of a three-layered device possessing two wide-band ChLC layers with birefringence of 0.20 was investigated at the same time. A series of spikes shows lasing from each cavity mode. In the device with two wide-band ChLC layers, lasing was observed from many cavity modes as 18 and the emission intesity at each cavity mode was determined only by fluorescence spectra. On the other hand, in the device with notch-ChLC layer, lasing only occurred from 6 cavity modes. In addition, a larger contrast was observed between the peak with the highest intensity and the adjacent modes. This result shows that the practically single-mode lasing in DBR-ChLC cavity with notch-ChLC layer is achieved due to its strong contrast of emission intensity (or lasing threshold) at each cavity mode.

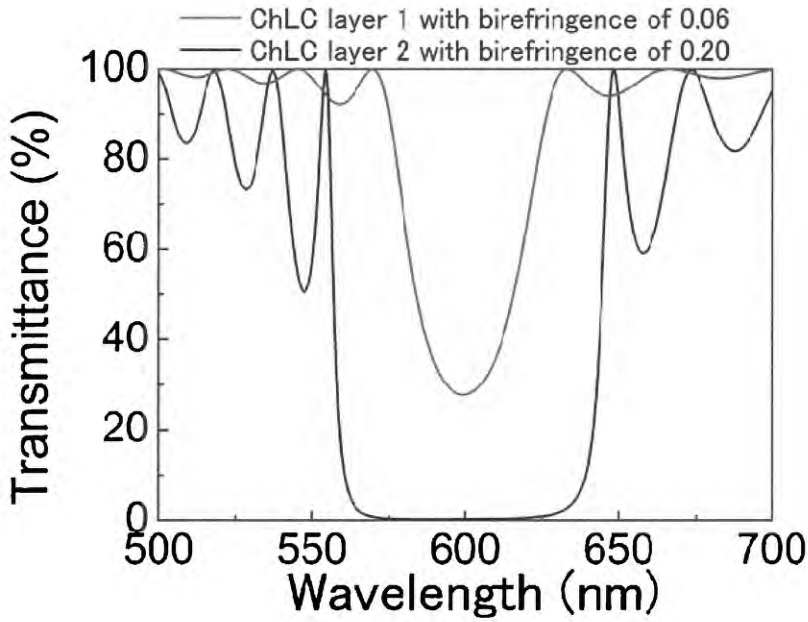

Fig. 2 Transmission spectra in the ChLC layer1 and 2 with birefringence of 0.06 and 0.20, respectively.

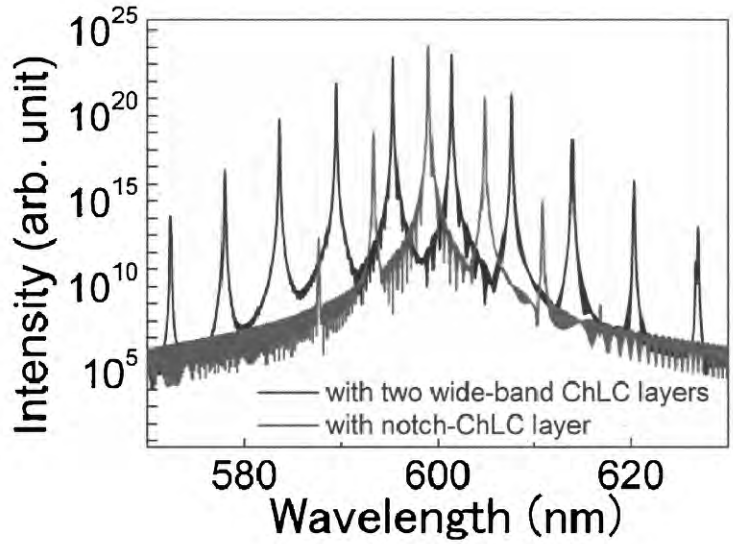

Fig. 3 Lasing spectra in the device possessing notch-ChLC layer and two flat-ChLC layers

Figure 4 shows lasing spectra from the DBR-ChLC cavity as the notch reflection band in the ChLC layer 1 was shifted. When the helical pitch of the notch-ChLC layer was varied, the reflection band was shifted based on the relation $\lambda_{lc} = \bar{n}p$ ($\bar{n} = \frac{n_{\parallel} + n_{\perp}}{2}$), where λ_{lc} is center wavelength of reflection band and $n_{\parallel}$ and $n_{\perp}$ are the refractive indices parallel and perpendicular to the LC director. Single-mode lasing was observed at each helical pitch of 388, 392, and 397 nm, and the lasing wavelength was shifted by the shift of the reflection band of the notch-ChLC, attributed to mode-hopping among the adjacent cavity modes.

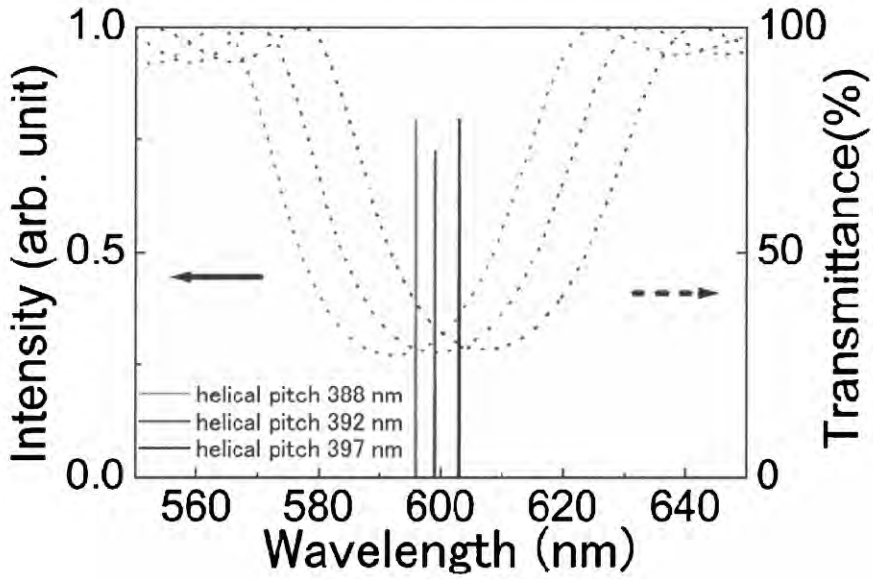

Fig. 4 Lasing spectra from the DBR-ChLC cavity as the notch reflection band was shifted

3. EXPERIMENTAL METHOD

In order to demonstrate tunable single-mode lasing observed in the simulation, the three-layered DBR-ChLC laser device schematically shown in Fig. 5 was fabricated. The right-handed PChLC material comprised two photopolymerizable ChLCs (90 wt% of 02-595, 10 wt% of 02-596) provided by Merck. The sample was placed in a sandwich cell with a cell gap of 16 μm and subjected to planar alignment treatment: each substrate was coated with polyimide (JSR AL1254) and rubbed unidirectionally. The material was cooled from above the clearing point (110 °C) to 60 °C before irradiating the cell with UV light (λ = 365 nm), and after polymerization, one of the substrates was removed. An ionic liquid [Kanto Chemical 1-allyl-3-butylimidazoliumbis(trifluoromethanesulfonyl)imide] was doped with 2-[6-(ethylamino)-3-(ethylimino)-2,7-dimethyl-3H-xanthen-9-yl] -benzoic acid (Exciton Rhodamine 6G) at a concentration of 0.5 wt% and used as the gain medium. The dye-doped ionic liquid was placed on top of the PChLC film and sandwiched with a 4-μm-thick polyethylene terephthalate (PET) film, using PET spacers of 16 μm thickness. The notch-ChLC, which was prepared by doping a right-handed chiral dopant (R811 Merck) in a low-birefringence (Δn=0.06) nematic host (Merck MLC-6881) at a concentration of 31 wt%, was then placed on top of the PET sheet and sandwiched with a glass substrate to a thickness of 4 μm. The glass substrate was covered with polyimide (JSR AL1254) and rubbed uniaxially to induce planar alignment at the substrate surface.

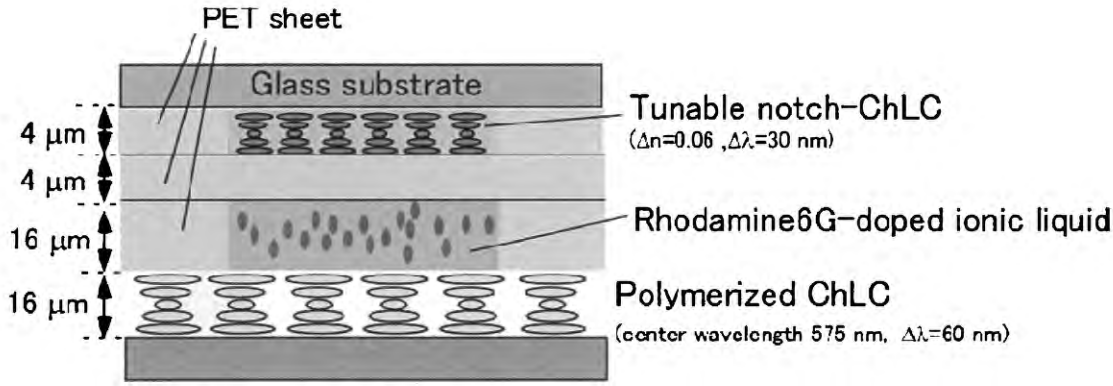

Fig. 5 Schematic of DBR-ChLC cavity with three-layered structure consisting of tunable notch-ChLC, wide-band PChLC reflectors, and dye-doped ionic liquid

4. EXPERIMENTAL RESULTS AND DISCUSSION

Figure 6 shows the reflection spectra of the PChLC layer and the notch-ChLC layer. The PChLC layer had a wide reflection band (Δλ=60 nm; center wavelength 575 nm) which was temperature-independent between 25.7 and 28.2 °C, while the notch-ChLC had a narrow reflection band (Δλ=30 nm) that blue-shifted continuously with increasing temperature. The difference in reflection bandwidth are attributed to the difference in the birefringence as explained in the simulation section.

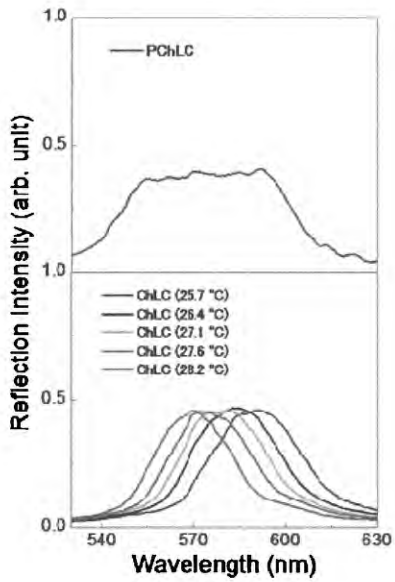

Fig. 6 Wide reflection band of the PChLC layer and notch reflection bands of the ChLC layer between 25.7 and 28.2 °C

A diode pumped, passively Q-switched, frequency-doubled Nd-doped yttrium alminum garnet laser (CryLas FDSS532-150) was used to excite the dye molecules doped in the ionic liquid: the wavelength, pulse width, and pulse repetition frequency were 532 nm, 1.5 ns, and 10 Hz, respectively. The excitation laser beam was focused over a circular area with a spot diameter of approximately 20 μm, and the emission spectrum was measured in the cell-normal direction through the notch-ChLC layer using a multichannel spectrometer (Hamamatsu PMA-11) with a spectral resolution of 2 nm. To evaluate the slope efficiency of the device, the average input and output powers were measured using a power meter calibrated to the detecting wavelength (Ophir PD300UV). The output power was also measured through the notch-ChLC layer. Also, for comparison to slope efficiency of the conventional DFB-ChLC lasers, a DFB-ChLC laser was prepared by doping a laser dye, 1,3,5,7,8-pentamethyl-2,6-di-t-butylpyrromethene-difluoroborate complex (Exciton pyrromethene 597) at concentration of 1.0 wt% in a ChLC prepared by adding a left-handed chiral dopant (Merck S-811) at a concentration of 32 wt% in a nematic LC host (Δn=0.262, Merck E-44). The pyrromethene-597-doped sample was infiltrated in a planarly-aligned sandwich cell with a thickness of 10 μm, following a previous study which reported the highest slope efficiency for this particular dye[12].

Figure 7 shows lasing spectra at various temperatures. Lasing occurred approximately from the wavelength at which the notch-ChLC reflection was highest. Tunable lasing was observed from the fabricated DBR-ChLC laser at various temperatures by mode-hopping, and also, clear single-mode lasing was achieved at each temperature.

Figure 8 shows the input-output characteristics of the rhodamine6G-doped DBR-ChLC and pyrromethene-597-doped DFB-ChLC laser. A slope efficiency of 16% was achieved in the DBR-ChLC laser, while the DFB-ChLC laser doped with pyrromethene 597 showed a slope efficiency of 11%. This improvement of slope efficiency in the DBR-ChLC laser is considered to be attributed to the quantum yield of laser dyes which is related to the rate of stimulated emission[13-15]: reported values of quantum yields for pyrromethene 597, and rhodamine 6G are appropriately 70 (in a nematic LC)[12] and 95% (in ethanol)[16], respectively. However, in terms of lasing threshold, threshold of the DBR-ChLC laser was 10 times higher than that of the DFB-ChLC laser. This result is thought to be due to the birefringence of the PET sheet, which causes degradation of Q-factor in the cavity because circular polarization confined in the DBR-ChLC cavity is converted into elliptical polarization by the refractive index anisotropy of the PET sheet. If the PET sheet can be removed by using a PChLC layer instead of the ChLC layer, improvements of lasing threshold in DBR-ChLC laser can be expected.

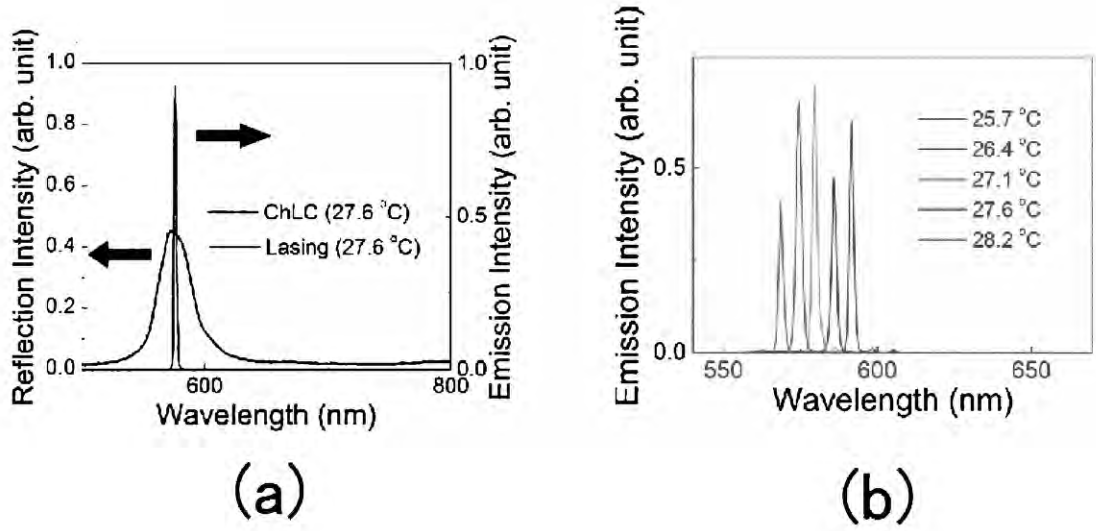

Fig. 7 (a) lasing spectrum at 27.6 °C and the reflection spectrum of the notch-ChLC at the corresponding temperature (b) Lasing spectra at various temperatures.

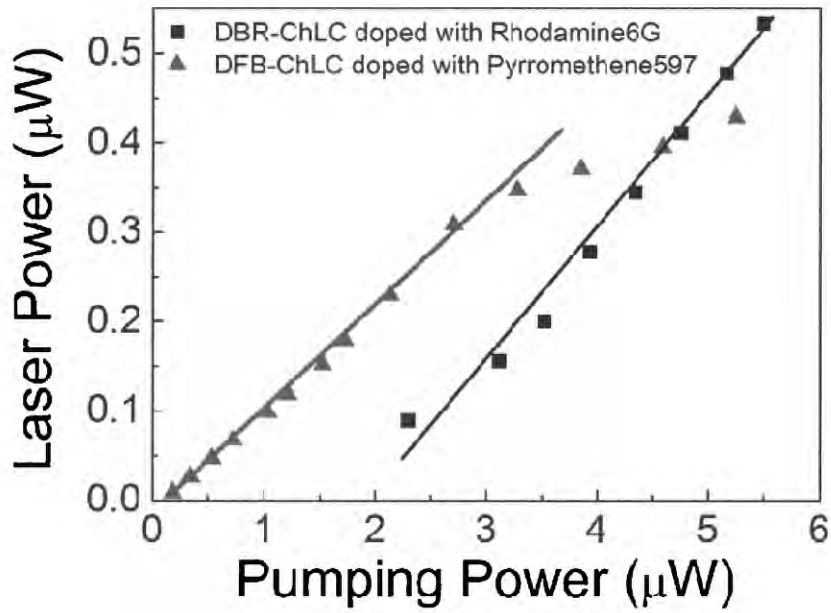

Fig. 8 Input-output characeristics of the DBR-ChLC laser doped with Rhodamine6G (0.5 wt %) and the conventional DFB-ChLC laser doped with pyrromethene597 (1.0 wt%).

5. CONCLUSION

We investigated lasing characteristics of the DBR-ChLC cavity with a three-layered structure consisting of an active layer and a notch-ChLC layer and a wide-band ChLC layer. In FDTD simulation, tunable single-mode lasing was predicted in the DBR-ChLC laser where active layer with thickness of 20 μm was sandwiched between a notch-ChLC and a wide-band ChLC with birefringence of 0.06 and 0.20. In experiment, also, tunable single-mode lasing was demonstrated using cavity mode hopping in a DBR-ChLC laser device where a dye-doped ionic liquid was sandwiched between a notch-ChLC and a wide-band PChLC with FWHMs of 30 and 60 nm, respectively. In addition, a slope efficiency of 16% was achieved for the Rhodamine-6G-doped DBR-ChLC laser, and was approximately 1.5 times larger than that of a 10-μm-thick DFB-ChLC laser doped with the pyrromethene 597 laser dye.

REFERENCES

[1] Coles, H. J. and S. M. Morris: "Liquid-crystal lasers," Nat. Photonics 4, 676–685 (2010).
[2] Funamoto, K., Ozaki, M., and Yoshino, K., " Discontinuous Shift of Lasing Wavelength with Temperature in Cholesteric Liquid Crystal," Jpn. J. Appl. Phys. 42, L1523-L1525 (2003).

[3] Finkelmann, H., Kim, S. T., Munoz, A., Palffy-Muhoray, P., and Taheri, B., " Tunable Mirrorless Lasing in Cholesteric Liquid Crystalline Elastomers," Adv. Mater. 13, 1069–1072 (2001).
[4] Araoka, F., Shin, K. C., Takanishi, Y., Ishikawa, K., and Takezoe, H., "How doping a cholesteric liquid crystal with polymeric dye improves an order parameter and makes possible low threshold lasing," J. Appl. Phys. 94, 279-283 (2003).
[5] Shibaev, P. V., Madsen, J., and Genack, A. Z., Chem. "Lasing and Narrowing of Spontaneous Emission from Responsive Cholesteric Films," Mater. 16, 1397-1399 (2004).
[6] Yoshida, H., Inoue, Y., Isomura, T., Matsuhisa, Y., Fujii, A., and Ozaki, M., "Position sensitive, continuous wavelength tunable laser based on photopolymerizable cholesteric liquid crystals with an in-plane helix alignment," Appl. Phys. Lett. 94, 093306 (2009).
[7] Inoue, Y., Yoshida, H., Inoue, K., Fujii, A., and Ozaki, M., "Improved Lasing Threshold of Cholesteric Liquid Crystal Lasers with In-Plane Helix Alignment," Appl. Phys. Express 3, 102702 (2010).
[8] Chilaya, G., Chanishvili, A., Petriashvili, G., Barberi, R., Cipparrone, G., Mazzulla, A., Desanto, M. P., Sellame, H., and Matranga, M. A., "Lasing in Three Layer Systems Consisting of Cholesteric Liquid Crystals and Dye Solution," Mol. Cryst. Liq. Cryst. 495, 97-105 (2008).
[9] Ha, N. Y., Jeong, S. M., Nishimura, S., Suzaki, G., Ishikawa, K., and Takezoe, H., "Simultaneous Red, Green, and Blue Lasing Emissions in a Single-Pitched Cholesteric Liquid-Crystal System," Adv. Mater. 20, 2503-2507 (2008).
[10] Berenger, J. P., "A perfectly matched layer for the absorption of electromagnetic waves," J. Comput. Phys. 114, 185 (1994).
[11]Yee, K. S., "Numerical solution of initial boundary value problems involving maxwell's equations in isotropic media," IEEE Trans. Antennas Propag. 14, 302-307 (1966).
[12] Mowatt, C., Morris, S. M., Song, M. H., Wilkinson, T. D., Friend, R. H., and Coles, H. J., "Comparison of the performance of photonic band-edge liquid crystal lasers using different dyes as the gain medium," J. Appl. Phys. 107, 043101 (2010).
[13] Sorokin. P. P., Lankard, J. R., Hammond, E. C., and Moruzzi, V. L., "Laser-pumped Stimulated Emission from Organic Dyes: Experimental Studies and Analytical Comparisons," IBM J. Res. Dev. 11, 130-148 (1967).
[14] Barroso, J., Costela, A., Garcia-Moreno, I., and Sastre, R., "Wavelength dependence of the nonlinear absorption properties of laser dyes in solid and liquid solutions," J. Chem. Phys. 238, 257-272 (1998).
[15] Parhat, H., Vasa, N. J., Kidosaki, M., Okada, T., Maeda, M., Mizunami, T., and Uchino, O., "Influence of a feedback coupling on operating characteristics of a Cr3+:LiSrAlF6 laser using an end-coupled fiber grating," Appl. Phys. B 70, 361-366 (2000).
[16] Magde, D., Wong, R., and Seybold, P. G., "Fluorescence quantum yields and their relation to lifetimes of rhodamine 6G and fluorescein in nine solvents: Improved absolute standards for quantum yields," Photochem. Photobiol. 75, 327-334 (2002).